Bu-Ali Sina University

Biosystems Engineering & Sustainable Technologies (BEST)

Journal Homepage: www.best.basu.ac.ir/
BEST J., 2(1) (2025) 51-60
DOI: https://doi.org/ 10.22084/best.2025.31612.1012

# Simulation of Compaction Behavior of Arable Soil by Finite Element Method with Mohr-Columb and Drucker-Prager Models

Maryam Biglari, Mojtaba Jaberi Moez*

*Department of Biosystems Engineering, Faculty of Agriculture, Bu-Ali Sina University, Hamedan, Iran.*

**PAPER INFO**

***Paper history:***
Received: Sep. 23, 2025
Revised: Nov. 11, 2025
Accepted: Nov. 30, 2025
Available Online: Dec. 30, 2025

***Keywords:***
Drucker–Prager
Mohr-Columb
Pre-Compression Stress
Plate Sinkage Test

**ABSTRACT**

Farm soil density affects the energy consumption of agricultural machinery and implements, root growth, and thus crop yield. Pre-compaction stress is one of the most important criteria for assessing soil compaction. The purpose of this study was to investigate the compaction behavior of a crop soil with sandy, clayey, and loamy textures during two tests of plate sinkage and compactness and They were simulated with Mohr-Columb and Drucker-Prager numerical models to evaluate the stress distribution and displacement in the depth and width of different soil layers and to predict soil compaction stress. During the experimental tests, the stress-displacement diagram of the soil compaction tests was drawn, and the pre-compression stress was determined by the Alexandro and Eral method from the plate subsidence test. The results showed that Drager-Prager and Mohr-Columb models with 99 and 98% explanation coefficient, respectively, were in good agreement with the data obtained from experimental experiments. The study of stress distribution and displacement in soil depth showed that the amount of stress and displacement in the layers close to the loading plate increased more, and the amount of stress and displacement decreased by moving to deeper layers. The simulation results also showed that the amount of stress across each layer of soil decreased with distance from the center of the loading axis. In the high-depth plate sinkage test, the depth stress distribution is almost fixed and negligible, while in the plate sinkage test and enclosed compaction (together), the amount of depth stress in the soil was fixed and stable. This indicates that the soil is compacted.

## 1. Introduction

Soil, as a natural resource, plays a crucial role in agriculture and food security. The physical degradation of soil structure by human activities is a global concern. Major factors contributing to soil physical degradation include compaction, waterlogging, and the subsidence of organic soils. Soil compaction is one of the main issues in modern agriculture, arising from the passage of agricultural machinery, and is recognized as a significant problem worldwide (Hamza & Anderson, 2005). A primary cause of compaction risk in agricultural soils is the mechanical pressure resulting from vehicle traffic in the field (Arvidson et al., 2011). Natural soil settlement, flood irrigation in soils with weak structure, and frequent traffic of heavy agricultural machinery across farmland are the main causes of soil compaction (Sivarajan et al., 2018).

Soil compaction reduces crop root growth and also leads to undesirable environmental effects such as reduced water infiltration into the soil profile, increased surface runoff during heavy rainfall, and ultimately soil erosion and the degradation of organic matter (Keller & Arvidson, 2004). In agricultural research, the concept of precompression stress is applied to describe the rapid compaction of unsaturated soils. Precompression stress is defined as the maximum stress a soil can withstand without undergoing additional compaction (Naderiboldaji et al., 2018). This parameter serves as a measure of soil strength for maintaining soil structure against internal and external forces (Gregory et al., 2006).

The main objective of determining precompression stress is to estimate soil bearing capacity or the stress threshold at which compaction occurs. By limiting applied loads (caused by machinery traffic) to values below the precompression stress, the risk of compaction (permanent deformation) can be minimized (Naderiboldaji et al., 2018). Experimental methods for measuring precompression stress include the oedometer test, confined compression test, semi-confined compression test, and plate loading test. However, research results indicate that even when stresses lower than the precompression stress are applied, significant permanent deformations may remain in the soil, suggesting that precompression stress is not always a reliable yield criterion (Keller et al., 2014).

*Corresponding author's email: m.jaberimoeaz@basu.ac.ir

Please cite this article as: Jaberi Moez, M., (2025). Simulation of Compaction Behavior of Arable Soil by Finite Element Method with Mohr-Columb and Drucker-Prager Models. *Biosystems Engineering & Sustainable Technologies (BEST), 2*(1), 55-64. https://doi.org/ 10.22084/best.2025.31612.1012

One of the effective approaches to investigate such problems is finite element simulation, which allows examination of the various factors influencing soil stress–strain behavior in uniaxial confined, semi-confined, and plate loading tests. This requires the application of appropriate models to predict soil behavior and to study different aspects and influencing parameters. From the perspective of soil management and crop production, the quality of tillage operations has always been a major consideration, with efforts directed toward designing implements and tools that minimize soil degradation and energy losses, which themselves entail both economic and environmental limitations (Peixoto et al., 2019).

Optimizing tillage tools and their modifications requires extensive testing under field conditions, which is costly and time-consuming. Therefore, numerical simulations provide a suitable alternative for optimization processes, reducing both experimental costs and research duration while offering accurate predictive models (Mardani et al., 2016). Compared to experimental and field methods, modeling approaches offer the advantage of precisely determining soil properties at any point and assessing the effect of different soil parameters on deformation and stress (Ucgul & Saunders, 2020).

For instance, Hemmat et al. (2010) simulated the stress–settlement behavior of clay loam soil in ANSYS software by considering linear viscoelastic soil behavior. Results indicated that the finite element method can effectively model soil settlement behavior. Mardani et al. (2016) analyzed tire–soil interaction using both numerical and experimental methods, investigating the effects of travel speed and dynamic tire load on vertical soil stress at various depths. In this study, soil was modeled as elasto-plastic and the tire as hyperelastic with limited strain. Similarly, Naderiboldaji et al. (2018) simulated uniaxial confined, semi-confined, and plate loading compression tests using the finite element method in ABAQUS software, modeling soil as an elasto-plastic material to study stress–strain curves and determine the point of maximum curvature relative to yield stress. Their results showed that increasing soil elasticity modulus and Poisson's ratio raises the precompression stress determined by the maximum curvature method, while increasing the internal friction angle (Drucker–Prager model) and piston penetration speed had no effect.

Given these studies, it is preferable to utilize various soil constitutive models in simulations and compare their results to select the most accurate one capable of describing all behavioral aspects and providing precise constitutive equations with improved numerical solutions. Such models can be effectively employed for combined plate loading and confined compression tests. Rashidi et al. (2010) simulated repeated plate loading tests using the finite element method, modeling soil in FLAC software as a linear elasto-plastic material. Experimental results demonstrated that the finite element method can relatively accurately represent soil settlement behavior under repeated loading.

Considering the importance of predicting pre-compression stress and understanding stress distribution and displacement under applied loads in soil compaction, the main objectives of this study are:

1. To perform experimental plate loading and combined plate loading–confined compression tests on an agricultural soil sample to evaluate its behavior and determine pre-compression stress.
2. To conduct finite element simulations of combined plate loading and confined compression tests, modeling soil as an elasto-plastic material and evaluating it using Drucker–Prager and Mohr–Coulomb failure criteria to analyze stress and displacement distribution across different soil layers in depth and width.

## 2. Materials and Methods

### 2.1. Soil Sample Preparation

This experiment was conducted at the research farm of Bu-Ali Sina University, Hamedan, Iran, located at 34°47′ N latitude, 48°28′ E longitude, and 1,844 m above sea level. To perform the experimental tests, soil samples were collected from the top 0-20 cm layer of the farm. The soil texture was classified as sandy clay loam, consisting of 46.82% sand, 27.28% silt, and 25.8% clay.

For bulk density measurement, a cylindrical container with a diameter of 20 cm and a height of 12 cm was used, yielding a bulk density of 1,500 kg·m³. Soil moisture content was determined by placing a 150 g sample in an oven at 5 ± 110 °C for 16 hours. The required amount of water to achieve the target gravimetric moisture content of 15% (d.b.) was calculated according to ASTM D2216. A thin soil layer was spread on a tray and uniformly moistened using a hand sprayer (Jaberimoeaz et al., 2017). Before sealing, the samples were placed in several plastic bags to preserve moisture. To homogenize moisture distribution, the samples were stored in sealed plastic bags for 24 hours (Hemmat et al., 2010). Subsequently, the required soil was weighed, divided into three equal parts, and each part was layered into the test container.

### 2.2. Experimental Tests

#### 2.2.1. Plate Sinkage Test and Confined Compression Test

The plate loading test was performed using a circular steel plate with a diameter of 50 mm and a thickness of 16 mm, applying load with a CBR testing machine at a rate of 1 mm·min$^{-1}$ (Jaberimoeaz et al., 2016). During the test, the loading plate was positioned at the center of the cylindrical soil container. Initially, the soil was loaded for 20 minutes, followed by a -30minute stabilization period before unloading. For each millimeter of settlement, the applied force was recorded using an S-shaped load cell, and a force–displacement curve was plotted. A settlement of 20 mm was considered the termination criterion of the test. Confined Compression Test is confined compression test *measures the capacity of a material to withstand axial compressive loads* without expanding perpendicularly to the force

### 2.2.2. Combined Plate Sinkage Test and Confined Compression Test

In the combined plate sinkage–confined compression test, soil loading was simultaneously applied using two circular steel plates: one with a diameter of 50 mm and a thickness of 16 mm, and the other with a diameter of 210 mm and a thickness of 16 mm, both operated with a CBR testing machine at a rate of 1 mm·min$^{-1}$. During the test, the 50 mm plate was applied first, followed by the 210 mm plate placed at the center of the soil container. Loading was continued until a total force of 487.4 kg was applied to the soil, after which the load was held constant for 30 minutes before unloading. For each millimeter of settlement, the applied force was recorded, and a force–displacement curve was generated. A settlement of 30 mm was considered the termination point of the test.

To determine Poisson's ratio and Young's modulus, a uniaxial compression test was conducted. Soil cohesion and internal friction angle were obtained from direct shear tests.

### 2.3. Determination of Soil Pre-compression Stress

The pre-compression stress was determined using the method proposed by Alexandru and Eral, based on the stress–settlement curve obtained from the plate load test. In this method, the intersection of two tangent lines to the stress–settlement curve indicates the preconsolidation stress. For this purpose, one tangent line is drawn from the origin of the curve, and the other tangent is drawn to the end portion of the curve. The intersection of these two lines determines the preconsolidation stress (Alexandru & Eral, 1995).

### 2.4. Finite Element Simulation of the Plate Load Test

To simulate the plate load test, ABAQUS version 14.6 was employed. The soil was modeled as a deformable two-dimensional body (a rectangle) with a height of 120 mm and a width of 105 mm, considering symmetry. Since the loading and boundary conditions were symmetric, half of the soil was modeled to simplify the process, and the results were generalized to the full soil geometry. The loading plate was modeled as a rigid body with a width of 25 mm, and the soil container was modeled as a rigid body with a height of 120 mm and a width of 105 mm in ABAQUS.

The geometric model of the plate load test and the combined confined compression test consisted of three parts: the soil body, the container, and the loading plate. The soil and the container were modeled in ABAQUS in the same way as in the plate load test.

In this study, the Mohr–Coulomb and linear Drucker–Prager models were used as soil failure criteria. The Drucker–Prager yield criterion is a pressure-dependent model for determining whether a material has failed or undergone plastic yielding. The criterion was introduced to deal with the plastic deformation of soils. It and its many variants have been applied to rock, concrete, polymers, foams, and other pressure-dependent materials. The yield functions of Mohr–Coulomb and linear Drucker–Prager are given in Equations (1) and (2), respectively (Tekeste et al., 2009):

In Equation (1), $c$ is cohesion, $\Phi$ is the internal friction angle, $\sigma n$ is the normal stress, and $\tau$ is the shear strength. In Equation (2), $t$ is the deviatoric stress (Pa), $p$ is the mean stress, $\beta$ is the angle of the linear yield function in the p–t stress plane, and $d$ is the intercept of the yield function in the p–t stress plane. The parameters $\beta$ and $d$ are analogous to the internal friction angle and cohesion in the Mohr–Coulomb criterion. $K$ is the ratio of the triaxial tensile yield stress to the triaxial compressive yield stress, which controls the dependency of the yield surface on the mean principal stress.

$$\tau = C + \sigma_n \tan\Phi \tag{1}$$

$$F = t - p\tan(\beta) - d = 0 \tag{2}$$

Given the internal friction angle of the soil (Φ), the value of $K$ can be calculated from Equation (3). The values of $d$ and $\beta$ are obtained from Equation (4).

$$K = \frac{3-\sin\phi}{3+\sin\phi} \tag{3}$$

$$\begin{cases} \tan\beta = \dfrac{6\sin\phi}{3-\sin\phi} \\ d = c\dfrac{6\cos\phi}{3-\sin\phi} \end{cases} \tag{4}$$

$\psi$ is the dilation angle, which determines the direction of plastic flow after failure. Equation (5) shows the relationship between the dilation angle and the internal friction angle in the Mohr–Coulomb model (Susila & Hryciw, 2003; Bolton, 1986):

$$\Phi = \Phi_{cv} + \psi \tag{5}$$

$\Phi cv$ is the constant-volume friction angle for soft granular materials. For finite element models, based on observations for sand and silica, its value was assumed to be 33° (Bolton, 1986).

The soil properties used for finite element simulation with the Mohr–Coulomb and Drucker–Prager models are given in Table 1.

### 2.5. Boundary Conditions and Meshing

To simulate the soil compaction test during both the PST and the combined plate load–confined compression test, the explicit dynamic method was used. To apply the load to the soil, in the plate load test, the loading plate was displaced vertically along the $y$-axis at a constant speed of 1 mm·min$^{1}$□,

**Table 1. Soil properties of the tested soil.**

| Density (kg·m⁻³) | Cohesion (kPa) | Internal Friction Angle (°) | Poisson's Ratio | Elastic Modulus (kPa) | d (kPa) | β (°) | K | ψ (°) |
|---|---|---|---|---|---|---|---|---|
| **1500** | 7.19 | 19 | 0.30 | 110 | 25.14 | 36 | 0.78 | 14 |

up to 20 mm. In the combined test, the loading plate was displaced 30 mm downward along the *y*-axis.

In both tests, the loading plate was constrained to move only along the *y*-axis, while its movements in other directions were fixed. The soil container was fully fixed in all directions. The central soil nodes along *x=0* on the *y*-axis were fixed in the *x*-direction, with their rotation about the *y*-axis restrained. The bottom soil nodes at *y=0* on the *x*-axis were restricted against movement in the *x*-direction but allowed to rotate about the *y*-axis.

A structured meshing technique was applied to discretize the soil domain using four-node axisymmetric linear elements (CAX4R).

## 2.6. Result and Discussion

Based on the results obtained from the soil behavioral models in the simulation of both the plate load test and the combined plate load–confined compression test, the Drucker–Prager behavioral model showed a better fit to the experimental data compared to the Mohr–Coulomb model, with a coefficient of determination of 99% (Fig. 1).

Figs. 2 and 3 show the stress–settlement curves of the soil obtained from finite element simulation of both tests compared to the experimental results. As can be seen from Figs. 2 and 3, the finite element method combined with the Drucker–Prager yield criterion accurately predicted the stress–settlement behavior of the soil beneath the loading plate during the soil compaction process. Therefore, the finite element method and the Drucker–Prager yield criterion can be reliably used to predict and analyze soil compaction behavior. Other researchers have also reported similar results when simulating soil compaction behavior using the Drucker–Prager model (Naderiboldaji et al., 2018).

## 2.6. Compressive Stress Distribution

If the stress at different soil depths under a loading factor is known, the degree of soil compaction can be estimated. In the present study, the stress distribution with depth was simulated using the proposed finite element model. The results from both the plate load test and the combined plate load–confined compression test are shown in Fig. 4.

By comparing the compressive stress distribution results in the soil layers for both tests shown in Fig. 4, it can be observed that in the plate load test, the highest stress occurs beneath and around the loading plate, while the stress at the edges of the soil is nearly zero. In contrast, in the combined plate load–confined compression test, stress is present throughout all soil layers, covering the entire soil surface. This

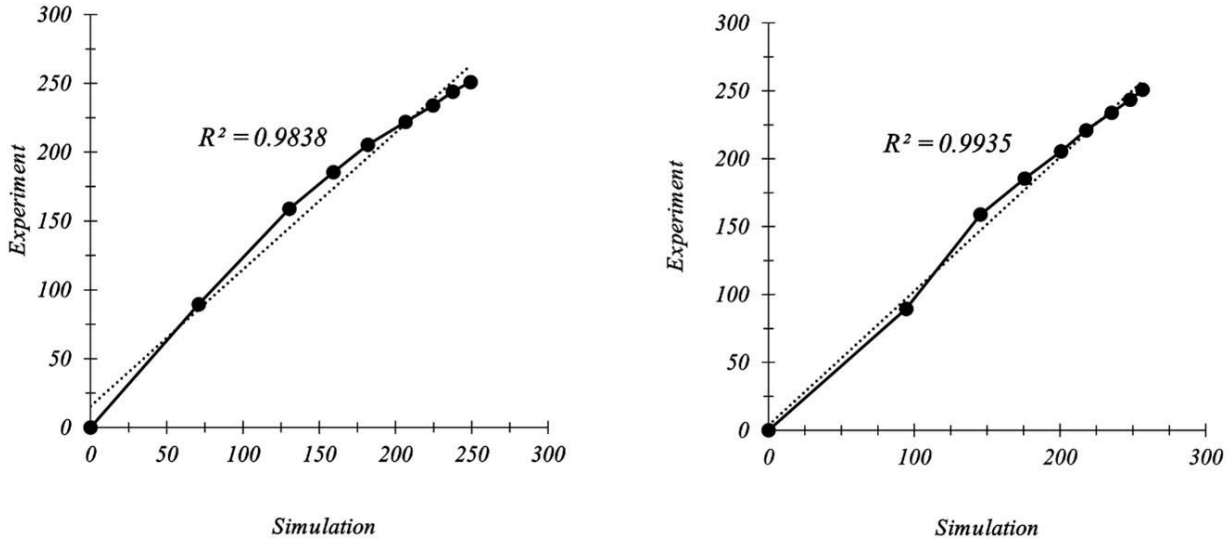


**Fig. 1. a: Coefficient of determination between experimental and simulated results in the plate load test; a: Drucker–Prager model, b: Mohr–Coulomb model.**

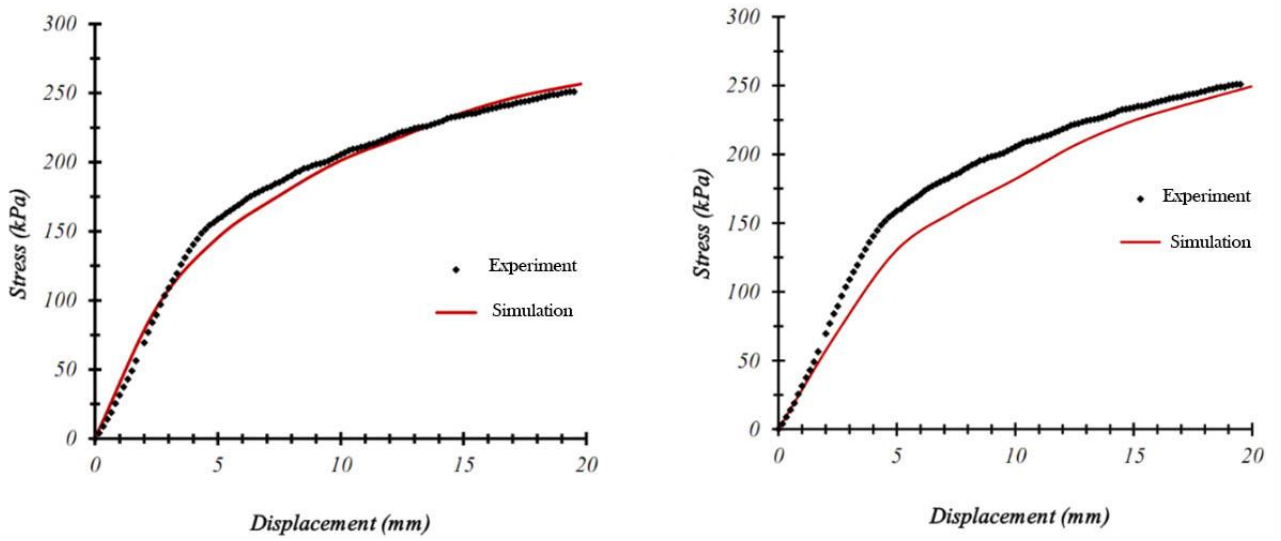


**Fig. 2. Comparison of stress–displacement results obtained from experimental tests and finite element simulation in the plate load test: a – with the Mohr–Coulomb yield criterion, b – with the Drucker–Prager yield criterion.**

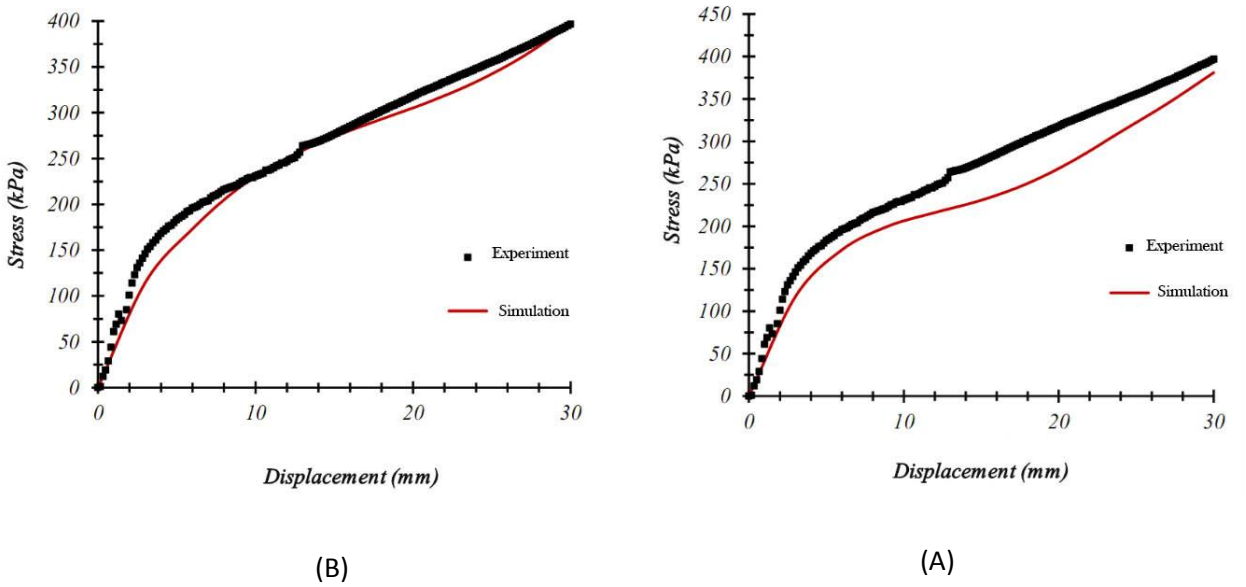


(B) (A)

**Fig. 3. Comparison of stress–displacement results obtained from experimental tests and finite element simulation in the combined plate load–confined compression test: A – with the Mohr–Coulomb yield criterion, B – with the Drucker–Prager yield criterion.**

difference in stress distribution between the two tests can be explained by the fact that in the plate load test, soil particles at the edges can move freely, whereas in the combined plate load–confined compression test, the soil is confined and particle movement is restricted. As a result, the stress from the applied load is not released by the soil particles, leading to residual compaction across all soil layers. The vertical stress distribution results using the Drucker–Prager and Mohr–Coulomb models are presented in Figs. 5 and 6.

As observed from the results in Figs 4 and 5, the vertical stress on the soil surface decreases as the distance from the point of applied axial load increases, and the horizontal stretching of the stress plot diminishes, approaching the vertical axis. The results indicate that applying an axial load increases stress in the soil, but the stress decreases with increasing depth. Habibi Bordbari et al. (2017) also reported that applying an overburden load increases the stress in the soil, and the effect of the load diminishes with distance both horizontally and vertically from the load application point.

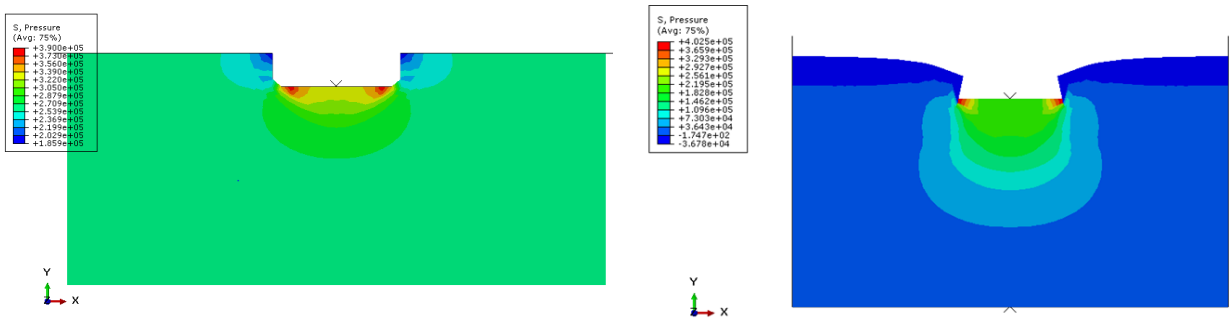

(B) (A)

**Fig. 4. Stress distribution in the soil at the end of the loading stage: a – plate Sinkage test, b – combined plate Sinkage test–confined compression test.**

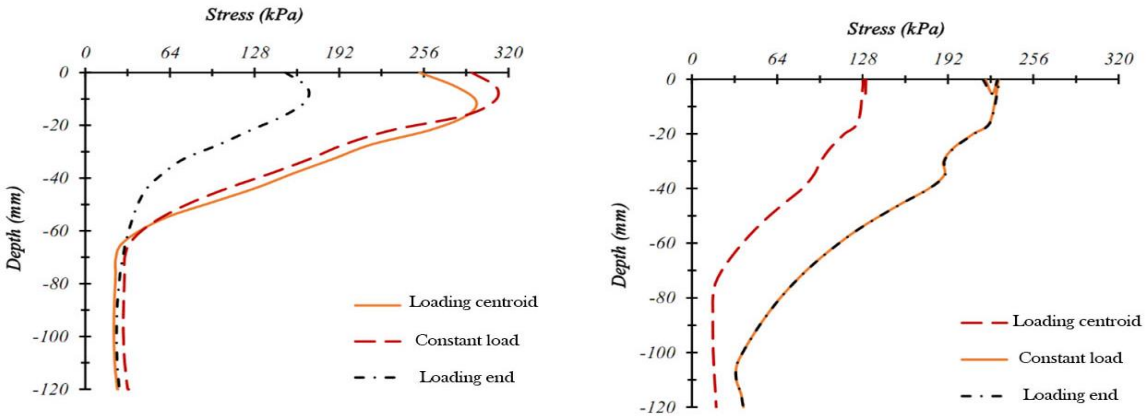


**(B) (A)**

**Fig. 5. Stress distribution with depth under axial load obtained from finite element simulation in the plate load test: a – with the Mohr–Coulomb yield criterion, b – with the Drucker–Prager yield criterion.**

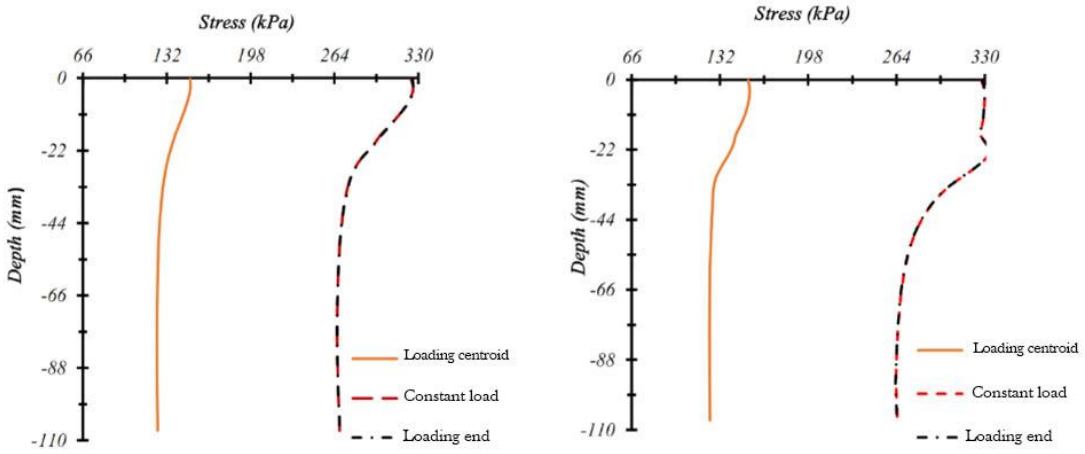


**(B) (A)**

**Fig. 6. Stress distribution with depth under axial load obtained from finite element simulation in the combined plate load–confined compression test: a – with the Mohr–Coulomb yield criterion, b – with the Drucker–Prager yield criterion.**

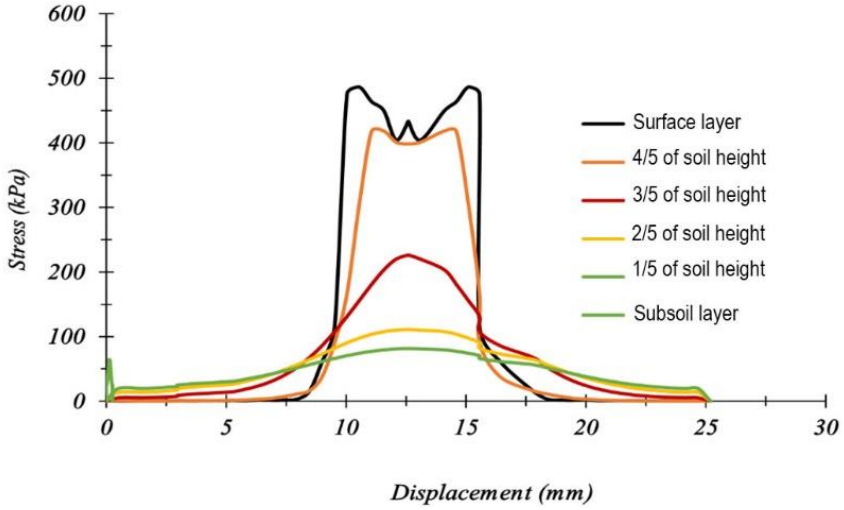


**Fig. 7. Horizontal stress distribution under axial load in the plate load test using the Drucker–Prager model.**

## 2.7. Stress Distribution in the Horizontal Direction

When an axial load is applied to the soil, the stress distribution across the soil width beneath and around the loading plate is considered. Due to stress concentration around the loading area during loading, the stress distribution is uneven, resulting in soil compaction beneath the loaded surface and around the load application point. The results of stress distribution across the soil width are presented in Fig. 7.

The results of this study regarding stress distribution with depth are consistent with those reported by Mardani et al. (2016) in their finite element analysis of the tire–soil interaction, which was conducted to estimate the vertical stress distribution in soil. Examination of vertical stress variations at different depths showed that results from both numerical and experimental methods, under various combinations of vertical load and travel speed, exhibited a power-law decrease in soil vertical stress with increasing depth. As soil depth increases, the load applied by the tire on the soil surface is dispersed. This bubble-like dispersion reduces the stress transmitted to the lower soil layers.

However, the present study indicated that stress reduction in the deeper soil layers did not occur in the combined plate load–confined compression test, and residual stress remained. The results obtained from the stress distribution with depth in the plate load test (Fig. 7) showed that stress decreased down to the lower soil layers, nearly reaching zero. This difference in stress can be explained by the fact that as the distance from the load application point increases, stress in the plate load test diminishes due to the smaller loading plate area and free edges of the soil surface, allowing soil particles to move and displace freely. In contrast, in the combined plate load–confined compression test, the loading plate covers the entire soil surface, and the soil is confined; thus, soil particles cannot move freely, resulting in higher stress in the lower layers compared to the plate load test, with stress remaining at the end of the loading stage.

Knowing the stress at any point within the loaded soil allows for determination of the load effect on the soil. During loading, care must be taken to ensure that the applied load does not cause soil compaction. If applying a load exceeding the soil's bearing capacity is unavoidable, the degree of compaction in different soil layers can be predicted. When using machinery and implements that exert compressive loads on the soil, it is crucial to ensure that compaction caused by axial compressive loads does not exceed the operational limits of tillage implements or the natural processes' tolerance. Otherwise, soil structure remediation costs will increase, and soil quality will decrease.

## 2.8. Soil Displacement Distribution

Fig. 8 shows the results of the simulated distribution of soil particle displacements in the vertical and horizontal layers of the soil at the end of the loading stage, obtained using the Drucker–Prager model.

With the vertical movement of the loading plate, soil particles are displaced in the vertical direction due to the force applied by the plate. This displacement consists of both plastic and elastic components; after unloading, the elastic portion of the vertical particle displacement recovers, leaving only the plastic displacement in the soil. Fig. 9 and 10 show the simulated soil displacement in depth using the Drucker–Prager and Mohr–Coulomb models.

As observed from Figs. 9 and 10, in the plate load test, with increasing distance from the center of the applied axial load towards the underlying layers, the displacement (deformation) in the soil decreases and eventually reaches zero. The results of this study showed that with increasing depth, the amount of settlement (compaction) due to the applied stress on the soil decreases. These findings are consistent with the results obtained by Sarbazvatan (2013) in measuring soil compaction under tractor tires using the finite element method with a modified Drucker–Prager

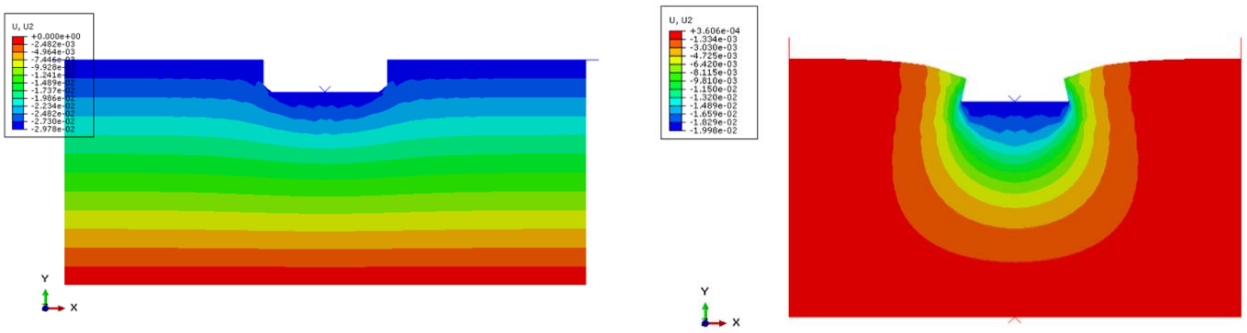

(B) (A)

**Fig. 8. Vertical deformation of soil layers in the tests: (a) Plate load test and (b) Combined plate load–confined compression test.**

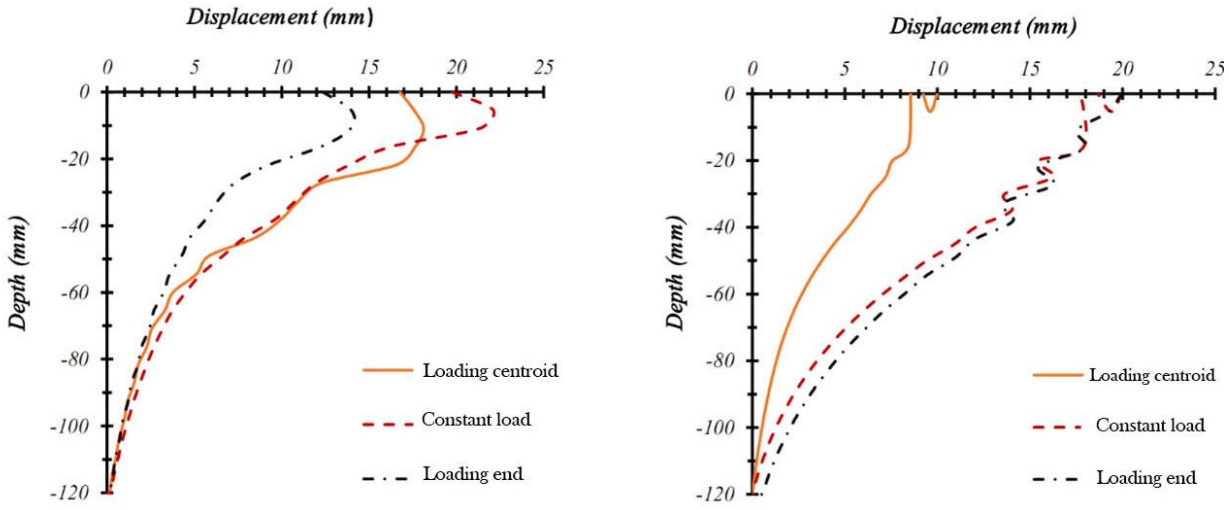


(B) (A)

**Fig. 9. Vertical displacement of soil layers in the plate load test: (a) Mohr–Coulomb criterion and (b) Drucker–Prager criterion.**

model, which indicated that the effect of the tire load on soil compaction decreases with depth.

The simulation results from the combined plate load and confined compression test showed that the soil surface under investigation, due to confinement beneath the loading surface, entirely entered the plastic phase, and the compaction covered the entire soil surface in this test. However, based on the results obtained from the plate load test, it was observed that the compaction created in the soil was mainly under the loading surface and around the load application area, and regions farther from the loading surface did not enter the plastic phase.

## 3. Overall Conclusion

The aim of this study was to investigate soil behavior during compaction operations and to evaluate it using failure analysis models in finite element simulations at a moisture content of d.b. 15%. It was determined that both the Drucker–Prager and Mohr–Coulomb models had good agreement with experimental results, with the Drucker–Prager model showing higher accuracy. The results indicated that with increasing load on the soil surface, the amount of stress and settlement increased, and the stress in deeper soil layers also increased. The stress and displacement were greater in layers near the

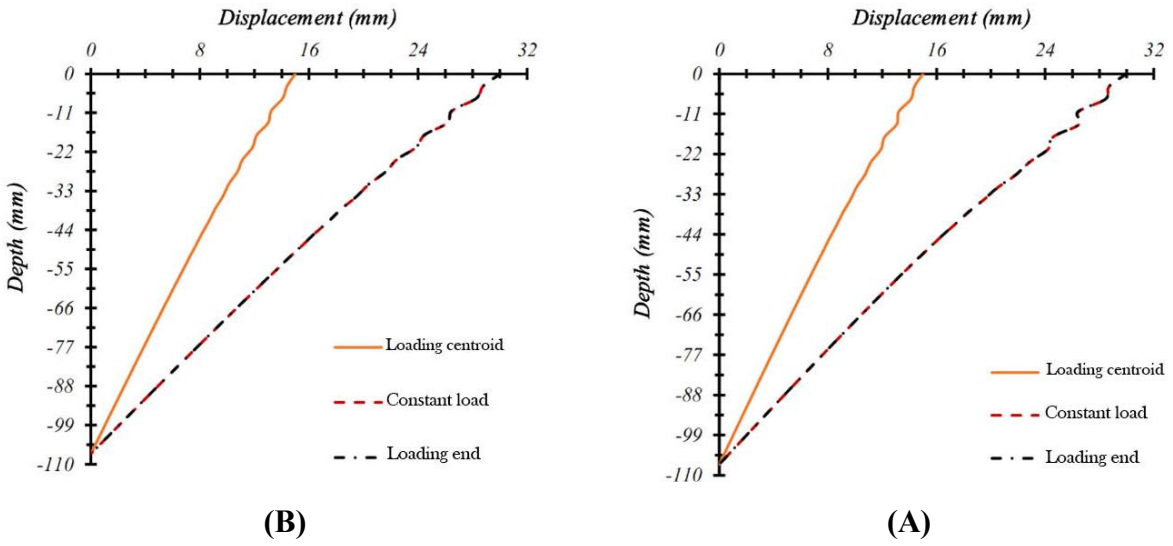


**Fig. 10. Vertical displacement of soil layers in the combined plate load–confined compression test: (a) Mohr–Coulomb criterion and (b) Drucker–Prager criterion.**

loading surface, and decreased toward the lower layers. The simulation results of the combined confined compression and plate load tests showed that with increasing depth beyond a certain point, the stress in the soil decreased, and in the lower soil layers, the stress stabilized, leaving residual stress. The stress distribution in the soil depends on the loading conditions and soil properties. The smaller the contact area of the applied axial load, the higher the stress generated in the soil, and the stress distribution assumes a parabolic shape.

## References


Alexandro, A., & Earl, R. (1995). In situ determination of the pre-compaction stress of a soil. *Journal of Agricultural Engineering Research, 61*(6), 71–77.

Arvidsson, J., Westlin, H., Keller, T., & Gilbertsson, M. (2011). Rubber track systems for conventional tractors: Effects on soil compaction and traction. *Soil and Tillage Research, 117*, 103–109.

Bolton, M. D. (1986). The strength and dilatancy of sands. *Geotechnique, 36*(1), 65–78.

Gregory, A. S., Whalley, W. R., Watts, C. W., Bird, N. R. A., Hallett, P. D., & Whitmore, A. P. (2006). Calculation of the compression index and precompression stress from soil compression test data. *Soil and Tillage Research, 89*(1), 45–57.

Habibi Bordbari, M., Zamanilanjani, M., & Parvizi, L. (2017). Analytical study and comparison of vertical stress distribution under loading of some cases located at the soil surface and depth. *International Civil Conference on Architecture and Urban Development Management* in Iran, University of Tehran.

Hamza, M., & Anderson, W. (2005). Soil compaction in cropping systems: A review of the nature, causes and possible solutions. *Soil and Tillage Research, 82*(2), 121–145.

Hemmat, A., Nankali, N., & Aghilinategh, N. (2010). Simulating stress–sinkage under a plate sinkage test using a viscoelastic 2D axisymmetric finite element soil model. *Soil and Tillage Research, 118*, 107–116.

Jaberimoez, M., Jafari, A., Keyhani, A., & Shorafa, M. (2017). Effect of freezing and thawing process on soil compaction. *Journal of Agricultural Mechanization, 4*(1).

Keller, T., & Arvidsson, J. (2004). Soil precompression stress: I. A survey of Swedish arable soils. *Soil and Tillage Research, 77*(1), 85–95.

Keller, T., Berli, M., Ruiz, S., Lamandé, M., Arvidsson, J., Schjønning, P., & Selvadurai, A. P. S. (2014). Transmission of vertical soil stress under agricultural tyres: Comparing measurements with simulations. *Soil and Tillage Research, 140*, 106–117.

Mardani, A., Dibagar, N., & Modaresmotlagh, A. (2016). Finite element analysis of drive-soil wheel interaction to estimate vertical soil stress distribution. *Agricultural Engineering, 39*, 113–125.

Naderi-Boldaji, M., Hajian, A., Ghanbarian, D., & Bahrami, M. (2018). Finite element simulation of plate sinkage, confined and semi-confined compression tests: A comparison of the response to yield stress. *Soil and Tillage Research, 179*, 63–70.

Peixoto, D. S., Silva, B. M., de Oliveira, G. C., Moreira, S. G., da Silva, F., & Curi, N. (2019). A soil compaction diagnosis method for occasional tillage recommendation under continuous no-tillage system in Brazil. *Soil and Tillage Research, 194*, 104–307.

Rashidi, M., Gholami, M., Ranjbar, I., & Abbassi, S. (2010). Finite element modeling of soil sinkage by multiple loadings. American-Eurasian *Journal of Agricultural and Environmental Sciences, 8*(3), 292–300.

Sarbazvatan, S. (2013). Measurement of soil compaction under tractor titration using finite element method (M.Sc. thesis). Department of Mechanical Engineering of Agricultural Machinery, Faculty of Agricultural Technology and Natural Resources, Mohaqiq Ardebili University.

Sivarajan, S., Maharlooei, M., Bajwa, S. G., & Nowatzki, J. (2018). Impact of soil compaction due to wheel traffic on corn and soybean growth, development and yield. *Soil and Tillage Research, 175*, 234–243.

Ucgul, M., & Saunders, C. (2020). Simulation of tillage forces and furrow profile during soil–mouldboard plough interaction using discrete element modelling. *Biosystems Engineering, 190*, 58–70.

Susila, E., & Hryciw, R. D. (2003). Large displacement FEM modeling of the cone penetration test (CPT) in normally consolidated soil. *International Journal for Numerical and Analytical Methods in Geomechanics, 27*, 585–602.

Tekeste, M. Z., Tollner, E. W., Raper, R. L., Way, T. R., & Johnson, C. E. (2009). Non-linear finite element analysis of cone penetration in layered sandy loam soil: Considering precompression stress state. *Journal of Terramechanics, 46*, 229–239.